JOURNAL OF Applied Polymer SCIENCE

Effect of the Unidirectional Drawing on the Thermal and Mechanical Properties of PLA Films with Different L-Isomer Content

J. C. Velazquez-Infante,[1] J. Gamez-Perez,[2] E. A. Franco-Urquiza,[1] O. O. Santana,[1] F. Carrasco,[3] M. Ll Maspoch[1]

[1]Centre Català del Plàstic (CCP), Universitat Politècnica de Catalunya, C/Colon 114, 08222 Terrassa, Spain
[2]Polymers and Advanced Materials Group (PIMA), Universidad Jaume I, 12071 Castelló, Spain
[3]Department of Chemical Engineering, Universitat de Girona, Campus de Montilivi, 17071 Girona, Spain
Correspondence to: J. Gamez-Perez (E-mail: jose.gamez@uji.es)

ABSTRACT: This work simulates the thermoforming process of two different L-isomer content PLA grades (95.6 and 98%), studying the influence on the induced morphology and the variation in the thermal and tensile properties. The thermoforming process was simulated with uniaxial tensile tests performed at different temperatures and strain rates, reporting the tensile behavior before, during, and after the test. The resulting structural changes were analyzed by wide-angle X-ray scattering and Fourier transformed infrared spectroscopy. Thermal characterization was carried out with differential scanning calorimetry and dynamomechanical thermal analysis. The results showed that, regardless the L-isomer content, drawing at 70°C produced a stable mesomorphic phase that showed greater tensile properties than the original films. This mesomorphic phase, indeed, could be reordered into a crystalline structure under mild annealing conditions (5 min/75°C), if compared with those needed for similar amorphous PLA specimens (60 min/120°C), thus providing a processing opportunity for obtaining thermally stable PLA products at temperatures above 100°C. © 2012 Wiley Periodicals, Inc. J. Appl. Polym. Sci. 000: 000–000, 2012

KEYWORDS: thermoforming; tensile properties; poly-lactic acid (PLA); mesomorphic phase

Received 21 November 2011; accepted 21 February 2012; published online
DOI: 10.1002/app.37546

INTRODUCTION

Currently, because of the ease of production, low cost, high production speed and volume, a great part of food packaging, which includes disposable plastics cups and containers, are shaped by thermoforming processes.[1] The most commonly used materials in the production of thermoformed plastic containers such as polystyrene (PS), polypropylene (PP), and acrilonitrile-butadiene-styrene have come, so far, from the petrochemical industry. At the end of their service life, high contamination in these containers precludes them from being recycled; in addition to their poor biodegradability, this leads to waste accumulation. A possible solution to this problem is to substitute these materials with biodegradable polymers.

Among biodegradable materials, polylactic acid (PLA) is one that has attracted the greatest interest because it is derived from renewable resources and can be processed easily.[2,3] This material is produced by active L and/or D lactic acid monomer condensation, which allows for obtaining a great number of stereo-copolymers through changing the L/D ratio in each material (i.e., varying the optical purity). It is well known that the properties of each PLA grade are strongly dependent on its optical purity, ranging from completely crystalline to completely amorphous materials.[4] With a glass transition temperature (T_g) between 50 and 70°C and a melt temperature (T_m) between 150 and 160°C, PLA slowly crystallizes from the melted polymer commonly found after processing in an amorphous state.[5] As a consequence, PLA shows a high brittleness and a low maximal temperature of use. Thus, improvements in these properties are required.[6,7]

It is known that polymer properties can be significantly enhanced through orientation processes. During stretching, polymer molecules are aligned, decreasing their configurational entropy, thus facilitating their incorporation into the crystalline phase, thereby increasing crystallinity (strain-induced crystallization).[8,9] It has been found that strain-induced crystallinity is a function of the thermoplastic system (polymer, stereoregularity, and additives) as well as the temperature and drawing rate and ratio. As a result, it is possible to obtain

© 2012 Wiley Periodicals, Inc.

materials with a wide range of properties by modifying the processing conditions.

As thermoforming is a thermally assisted deformation process in which a plastic sheet is heated and shaped, the polymer may acquire different degrees of orientation during the different processing stages. Therefore, the strain-induced crystallization phenomenon can occur, affecting to biodegradability[10] or mechanical properties[11–13] of PLA. Therefore, understanding the behavior of the material during and after deformation is key to the process. Also, it is well known that the drawing stage for a polymer without a well-defined yield point area is more gradual and leads to parts with smaller wall thickness variations,[8,14] being the minimum temperature required to perform the thermoforming process the one at which such behavior occurs. Therefore, it is important to obtain the shape of the stress–strain curves as a way to determine the conditions under which the material exhibits an ambiguous yield point. One of the purposes in this work is to report the uniaxial tensile and preliminary thermoforming behavior of a selected number of extruded sheets of two different L-isomer content PLA (96% and 98%).

Studies on the PLA process-induced morphology have been mostly related to fiber orientation[13,15] and, to a lesser extent, on the orientation of films.[10,12,16] In terms of fiber orientation, it has been found that the crystallinity and the degree of molecular orientation increase with increased drawing speed.[15] On the other hand, Lee et al.[10] studied the structure developed by uniaxial stretching of PLA films, both amorphous and crystalline. In amorphous PLA samples, they concluded that the degree of orientation increases with decreasing stretching temperature. Decreasing drawing temperature seems to hinder molecular relaxation processes, leading to more uniform orientation. But for precrystallized samples, it was found that the degree of orientation increases with increased temperature because of greater spherulite deformation. However, most of those studies are mainly focused on the development of the structure induced by the orientation rather than describing in detail its impact on the final mechanical properties.

In a previous work, Yu et al.[12] concluded that film orientation promoted during the melt stage of the extrusion line had no significant effects on the mechanical properties, whereas orientation induced in a second stage above glass transition temperature (T_g) resulted in an increase in stiffness and strength related with an increase on the crystallinity ratio. Stoclet et al.[16,17] proposed the development of a metastable phase (mesomorphic phase) to explain the mechanical and thermal behavior of those PLA sheets.

In this work, the thermal and mechanical behavior of films produced from two commercial grades of PLA and subjected to different strain rates and temperature conditions has been studied. We report the influence of the L-monomer content, strain rate, and final deformation on the thermomechanical properties of specimens obtained simulating a thermoforming process. The purpose of this study is to evaluate the influence of the crystallinity developed during thermoforming-like conditions on the thermal stability and tensile properties of the samples, as well as to study how they are affected by the L/D monomer ratio present in the PLA.

EXPERIMENTAL

Materials

Two commercial PLA grades from Natureworks® with 95.8 and 98% L-lactic isomer content were used: PLA 2002D (from now on PLA96) and PLA 4032D (from now on PLA98), respectively.[18]

Film Preparation

Materials were first dried in a PIOVAN (DSN-560HE, Italy) dehumidifier, with a dew point of −40°C, at 80°C for 3 h. Films were then prepared by cast extrusion in a single-screw extruder Collin Teach-Line™ E16T ($L/D = 25$; $D = 16$ mm) with a 100 mm flat die and 0.35 mm lips opening. The temperature profile varied from 145 and 190°C in the barrel and 200°C at the die. The extrudate was cooled on chill rolls (Collin Teach-Line TM CR72T, Germany) at 50°C, yielding a uniform film with a nominal thickness of 0.30 mm.

Mechanical Characterization

The mechanical behavior was determined by uniaxial testing, performed at different temperatures and testing rates. Tests were carried out using a Sun2500 (Galdabini, Italy) universal testing machine, equipped with a thermal chamber Eurotherm 2408 (Eurotherm SpA, Italy), a 1 kN load cell and a video extensometer (Mintron OS-65D, Taipei). ASTM type IVA dog-bone specimens, parallel to the extrusion machine direction (MD), were die punched from the films. Before testing, the specimens were equilibrated by placing them in the thermal chamber at their testing temperature (22, 50, and 70°C) for 10 min before tensile loading. Tensile crosshead rates were 1, 10, and 100 mm/min and drawing continued through the yield point up to the specimen failure or to maximum range of the testing machine moving clamp.

From the obtained stress–strain curves, the Young's modulus (E), yielding stress (σ_y), strain at yielding (ε_y), and strain at break (ε_b) were assessed, averaging at least five valid specimens.

Thermal Characterization

The thermal properties were determined by differential scanning calorimetry (DSC), in a Perkin Elmer Pyris 1 calorimeter, with an Intracooler Perkin 20 cooling system. Samples of 10 mg was heated in aluminum pans from 30 to 200°C at a heating rate of 10°C/min under a nitrogen atmosphere. The temperature and the heating flow scales were calibrated with indium and tin, using the standard procedure ASTM D7426. The glass transition temperature (T_g), the cold crystallization temperature (T_{cc}), and the melting temperature (T_m) were determined from the thermograms. Enthalpies corresponding to molecular relaxation after T_g (ΔH_{rel}), cold crystallization (ΔH_{cc}), and melting (ΔH_m) were also assessed.

The crystalline weight fraction (X_c) of the samples was determined by taking into account the cold crystallization of poly(L-lactic acid):

$$X_c = \frac{\Delta H_m - \Delta H_{cc}}{\Delta H^o} \times 100 \quad (1)$$

where ΔH^o is the heat of fusion of a theoretically 100% crystalline PLA sample, i.e., 93 J/g.[19]

Fourier Transformed Infrared Spectroscopy

Infrared spectra of the films were determined using a Nicolet 6700 FTIR spectrophotometer, using a Smart Orbit ATR accessory with a diamond disc. The number of scans was 32, with a wavelength resolution of 4 cm^{-1}

Dynamomechanical Thermal Analysis

Dynamic mechanical properties of all samples were measured with a Q800 DMA analyzer (TA Instruments-Waters LLC, United Kingdom) in a tensile mode. Test samples of 35 × 6 mm^2 (height × width) were used. The dynamic storage moduli (E') were determined at a constant frequency of 1 Hz and a heating rate of 2°C/min as a function of temperature from 30 to 160°C.

Wide-Angle X-ray Scattering

Wide-angle X-ray scattering experiments (WAXS) were performed using a Bruker AXS D4 Endeavour diffractometer. Scans of transmitted intensity versus scattering angle (2θ) were recorded at room temperature in the range 5–30° (step size = 0.02 (2θ), scanning rate = 8 s/step) with identical setting of the instrument by using filtered CuK_α radiation (λ = 1.54 Å), an operating voltage of 40 kV, and a filament current of 30 mA.

Thermoforming Simulation

The thermoforming process was simulated by uniaxial tensile drawing using a universal testing machine equipped with a thermal chamber. Rectangular specimens of 125 × 40 mm^2 cut along the MD direction were drawn at 70°C up to 200% strain (initial gauge length was 65 mm). After drawing, the films were fast cooled while they were still under stress. Such stretched films will be referred to in this work as st-PLA96 and st-PLA98 to differentiate them from their corresponding original films.

RESULTS AND DISCUSSION

Influence of the L-Isomer Content on the Thermomechanical Behavior

Figure 1 shows the DSC thermograms corresponding to the first heating of the films. In both curves, an endothermic sign can be observed at about 60°C, just after the middle point glass transition temperature (T_g). This is a typical response of physically aged polymers and is caused by a slight rearrangement of the polymer chains toward thermodynamic equilibrium that leads to a decrease in the free volume and a decrease in segmental mobility, with a small densification of the material. Upon heating, when the chain mobility increases, the polymer chains undergo a molecular relaxation phenomenon with heat absorption (ΔH_{rel})[20,21] as shown in DSC thermograms, just after T_g. This physical aging phenomenon is accompanied by an increase on stiffness and brittleness on the tensile properties of PLA.[6]

In the curve corresponding to PLA98 (with a D-isomer content of 2%), an exothermal signal can also be seen, which corresponds to cold crystallization. On the other hand, PLA96, with a D-isomer content of only 4.25%, did not show cold crystallization. It is known that the PLA trend to cold crystallization during heating depends on its stereoregularity (i.e., the optical purity or L-isomer content)[22]; for a heating rate of 10°C/min, only PLA98 shows a significant cold crystallization phenomenon.

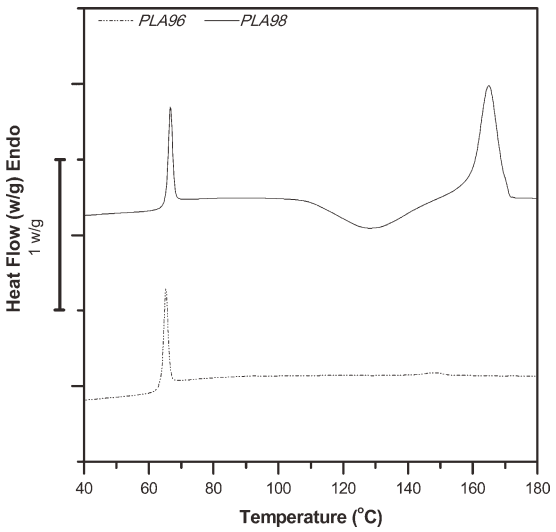

Figure 1. Thermograms corresponding to the first heating ramp of PLA96 and PLA98 films.

The endothermic signal observed at temperatures ranging from 150 to 170°C was attributed mainly to the melting of the PLA crystals, some of them developed during cold crystallization. The peak melting temperature is related to the lamellar thickness of the crystals; the presence of optical impurities in PLA produces curled and thin lamellae, which completely hamper the crystallization ability of PLA.[23] This endotherm shows highest intensity in the case of PLA98, indicating that a significant amount of thick crystals. The estimated degree of crystallinity (X_c) of the films, after correction for cold crystallization enthalpy, was 0.9 and 4.2 for PLA96 and PLA98, respectively. These values indicate that the films were essentially amorphous, with some crystals formed in the case of PLA98 due to its greater stereoregularity.

Regarding the mechanical tensile behavior, Figure 2 shows the stress–strain curves obtained for both films. In these curves, a similar tensile behavior can be observed. Nevertheless, there are some small variations in the tensile strength (σ_y) and stress at break (σ_b), which can be attributed to the differences in X_c. Yielding in both cases took place without necking formation or showing crazes through the calibrated portion of the specimen. Afterwards, stress was stabilized until brittle catastrophic failure at strain values near 15%.

Uniaxial Drawing at Different Rates and Temperatures

Even though during the initial free deformation stage of the thermoforming process, the sheet is typically biaxial stretched and undergoes unconstrained deformation; when the sheet contacts the mold surface, the initiation of stretching may be predominantly subjected to uniaxial deformation. Because of the complexity derived from the consideration of a biaxial deformation process, simpler uniaxial tensile deformation was first investigated in this study, by varying the temperature and testing rate. The results of the tensile properties and thermal behavior assessed by the DSC experiments are summarized in Tables I and II.

Applied Polymer SCIENCE

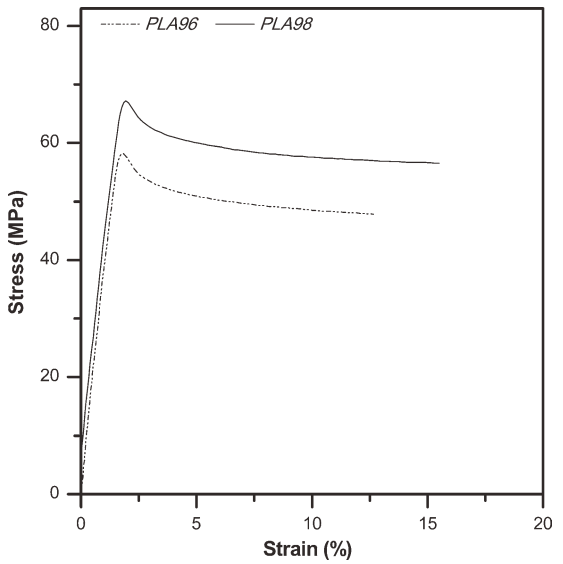

Figure 2. Stress–strain curves of PLA96 and PLA98 films, tested at 22°C and 10 mm/min.

Influence of Temperature on Tensile Behavior. Three different temperatures were used in tensile test: room temperature and 10 degrees (approx.) below and above T_g (23, 50, and 70°C, respectively) at a drawing rate of 10 mm/min. The assessed tensile parameters from the stress–strain curves are reported in Table I.

As expected, a sharp change in the tensile behavior below and above T_g was found. The increase in temperature from 23 to 50°C produced a decrease in σ_y and E. Nevertheless, films exhibited in both cases a sudden brittle failure, as can be deduced from their low values of strain at break (ε_b). On the other hand, at 70°C, completely ductile behavior with no rupture at strains of 400% strain characterized the tensile behavior of the films, with a drastic drop in σ_y and E. Therefore, a temperature of 70°C, which allows for obtaining high strain values with low stress levels, was the one chosen for simulating the thermoforming process.

Effect of Strain Rate on Mechanical Behavior, Thermal Properties, and Crystal Structure. The tensile properties of the films at 70°C were determined by varying the crosshead testing rate at 1, 10, and 100 mm/min, which produced initial deformation rates of 0.00031, 0.0032, and 0.033 s^{-1}, respectively. In Figure 3, the representative stress–strain curves of PLA96 (a) and PLA98 (b) are plotted at those testing rates. In both cases, there was a common gradual drawing process without showing a sharply defined yielding area, located in the strain range between 50 and 100%, depending on the testing rate.

After yielding, the curves showed a strain-hardening phenomenon, which was related to strain orientation and crystallization. Such behavior is desirable in industrial thermoforming processes because it helps to obtain high quality pieces with small thickness variations ("self-level").[8] At crosshead rates of 10 mm/min and higher, the start of the strain hardening phenomenon was shifted toward lower draw ratio values. It is worthwhile to highlight that PLA98 tested at 1 mm/min showed, unexpectedly,

Table I. Test Conditions and Mechanical Parameters from Tensile Tests

Sample	Test rate (mm/min)	22°C				50°C				70°C			
		E (GPa)	σ_y (MPa)	ε_y (%)	ε_b (%)	E (GPa)	σ_y (MPa)	ε_y (%)	ε_b (%)	E (GPa)	σ_y (MPa)	ε_y (%)	ε_b (%)
PLA96	1	3.7 ± 0.1	56.2 ± 0.7	1.6 ± 0.1	24 ± 5	[a]	[a]	[a]	[a]	2.9×10^{-3} ± 0.4	0.7 ± 0.01	100 ± 1	[a]
	10	3.9 ± 0.1	60.2 ± 2.6	1.8 ± 0.1	13 ± 2	3.7 ± 0.1	45.8 ± 0.6	1.9 ± 0.2	45 ± 12	3.0×10^{-3} ± 0.2	1.1 ± 0.04	120 ± 1	[a]
	100	4.0 ± 0.1	67.2 ± 1.0	2.1 ± 0.1	8 ± 0.4	[a]	[a]	[a]	[a]	3.5×10^{-3} ± 0.2	1.6 ± 0.04	149 ± 2	[a]
PLA98	1	3.7 ± 0.1	58.4 ± 0.7	1.6 ± 0.1	17 ± 4	[a]	[a]	[a]	[a]	3.1×10^{-3} ± 0.03	0.8 ± 0.1	76 ± 3	[a]
	10	3.9 ± 0.1	68.1 ± 0.6	2.1 ± 0.1	16 ± 0.4	3.4 ± 0.2	46.7 ± 1.0	1.9 ± 0.2	27 ± 8	3.5×10^{-3} ± 0.3	1.1 ± 0.1	99 ± 6	[a]
	100	4.0 ± 0.1	71.3 ± 2.7	2.6 ± 0.2	6 ± 0.4	[a]	[a]	[a]	[a]	4.0×10^{-3} ± 0.05	1.6 ± 0.2	107 ± 7	[a]
St-PLA96	10	4.5 ± 0.2	102.7 ± 2.4	3.3 ± 0.2	57 ± 3	[a]	[a]	[a]	[a]	[a]	[a]	[a]	[a]
St-PLA98	10	5.2 ± 0.4	117.5 ± 3.6	3.0 ± 0.1	36 ± 3	[a]	[a]	[a]	[a]	[a]	[a]	[a]	[a]

[a]Not evaluated.

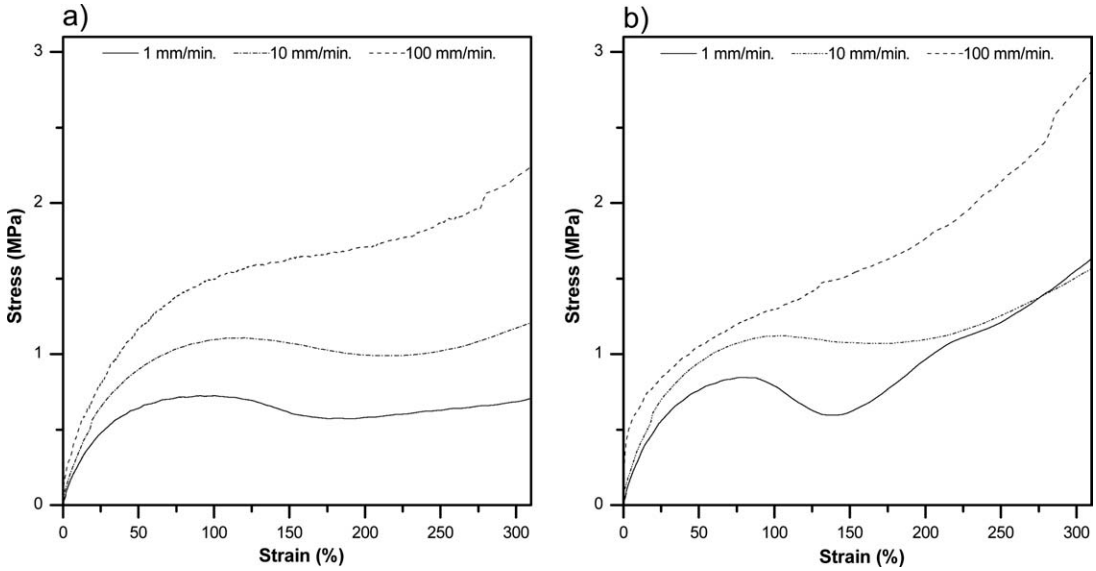

Figure 3. Stress–strain curves at 70°C and different strain rates: PLA96 (a) and PLA98 (b).

the same hardening rate as PLA98 tested at 100 mm/min. In fact, at 1 mm/min, the test took 80 min to complete, which is the equivalent of a thermal annealing process.[24,25] It can be deduced that at this temperature, crystallization is promoted by two different mechanisms: strain orientation and thermal annealing.

Specimens of PLA98 and PLA96 tested at 70°C showed similar yielding stress values at similar testing rates, as shown in Figure 4. PLA98 films, however, showed a higher elastic modulus than their corresponding PLA96 samples. Also in this figure, a linear trend of both tensile parameters (E and σ_y) with the logarithm of the testing rate can be assessed, which is of special interest for predicting the tensile behavior at intermediate rates.

After drawing the films at 70°C and different strain rates, the differences in the crystalline structure were investigated. During a typical thermoforming process, some areas may present different degrees of strain and/or strain rate,[26] depending on the thickness and shape of the molded object. Therefore, it may be expected that the thermal and mechanical properties will not be uniform, but variable. For such a reason, the thermal properties were assessed at different strain rates and draw ratios from the central part of tested tensile specimens at 70°C. Figure 5(a,b) show the first heating scans of the samples strained at 200% at different crosshead rates for PLA96 and PLA98, respectively. These thermograms confirmed the presence of structural variations as a function of the L/D ratio and the strain rate, especially with respect to the unstrained films. In Figure 5(a), all stretched PLA96 specimens show an exothermic signal that may be related to cold crystallization, not present in the original film [Figure 1(a)].

As the testing rate increased, the peak-temperature of that exothermic peak was shifted to lower values, down to 75°C at 100 mm/min. It can be remarked that in the case of PLA98, for the films strained at 1 mm/min, the thermogram did not show such peak, in agreement with the previous hypothesis that the film would have annealed during the test.[27] On the other hand, PLA98 films, strained at 10 and 100 mm/min, showed similar behavior as PLA96 films, also with an exothermic peak at 75°C.

All the data from the first heating scans of the unstrained films and samples strained at 200% are summarized in Table II. Thermal data from samples that were strained at 400% or thermally annealed are also included in Table II and will be discussed in further sections.

The results show that drawing, in all cases, had an influence on the glass transition area and on the apparent content of crystalline phase present. T_g decreased as the drawing rate increased, from 65 to 66°C (original films) to about 62°C in drawn

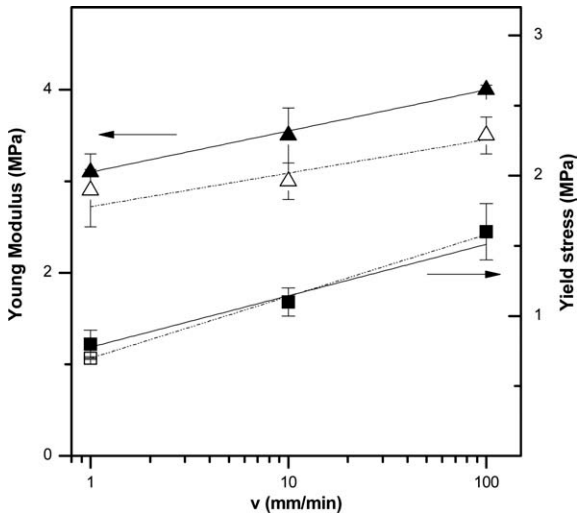

Figure 4. Young's Modulus (E) and yield stress (σ_y) as a function of the strain rate at 70°C: PLA96 (empty symbols) and PLA98 (filled symbols).

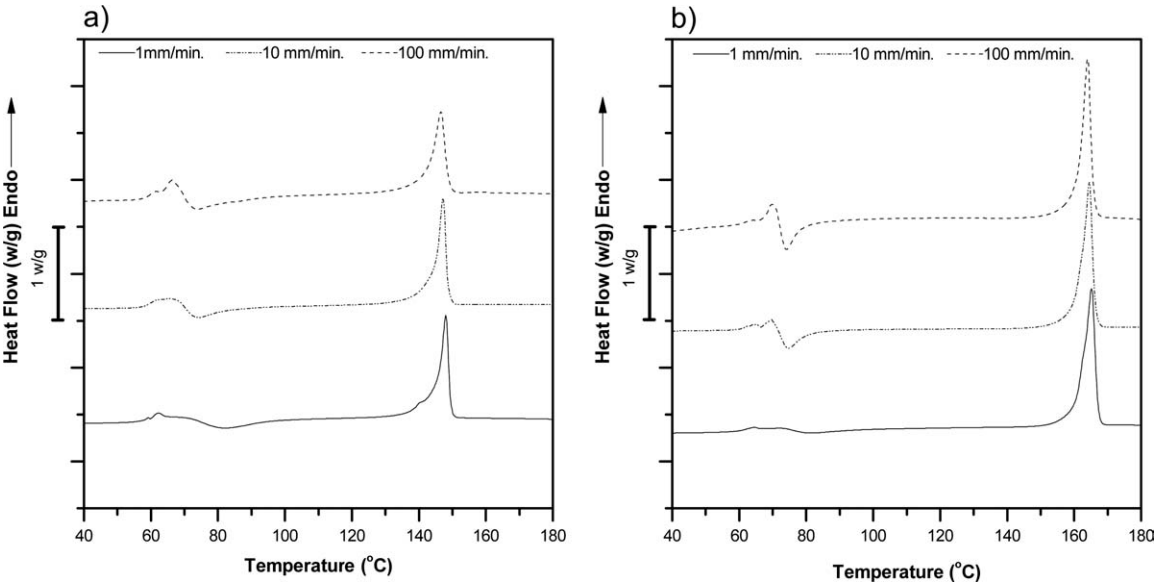

Figure 5. Thermograms showing the first heating ramp of the stretched zone in postmortem tensile specimens of PLA96 (a) and PLA98 (b). Tensile tests were carried out at 70°C and different crosshead rates.

samples at 100 mm/min. However, the relaxation enthalpy (ΔH_{rel}) decreased with increasing the testing rate, showing a trend that can be related with the time that the samples were inside the thermal chamber during the tensile test: the slowest testing rates (where the samples stayed more time at 70°C) are associated with lower ΔH_{rel} values.

It can also be seen that the drawing ratio on the specimens drawn at 100 mm/min (100% and 200%) did not produce significant variations in thermal behavior, regardless of the L/D monomer ratio, as shown in Table II. On the other hand, it can be affirmed that drawing promoted an apparent significant increase in X_c, regardless of the strain rate. This apparent increase in X_c, according to the DSC data, was about 20% for PLA96 and 30% for PLA98.

When the drawn films were analyzed by wide-angle X-ray diffraction, however, the spectra corresponding to stretched films (200%, 100 mm/min) did not show clear diffraction peaks, as one could expect from such values of crystallinity. Those films showed instead only a wide broad peak with very low diffraction intensity at $2\theta = 16.3$, as shown in Figure 6. In contrast, a sample of a thermally annealed film (110°C for 6 h–PLA96-*ntA*) is shown, which yielded a X_c value of 31.5% assessed by DSC (Table II). The estimated crystallinity of the stretched films by WAXS, reported in Table II, show contradictions with respect to the X_c values assessed by DSC.

Such a disagreement could be explained if we consider that most of the final crystalline structure seen in the stretched films by DSC scans developed during the heating step, at

Table II. Thermal Properties Determined from First Heating Thermograms of Samples Before and After Being Subjected to Different Stretching Process

Material			Thermal properties						
Sample	Test rate (mm/min)	ε (%)	T_g (°C)	ΔH_{rel} (J/g)	T_{cc} (°C)	ΔH_{cc} (J/g)	T_m (°C)	ΔH_m (J/g)	X_c (%)
PLA96	nt	0	65	6.0	–	–	148	0.8	0.9
	nt-A	0	62	0.8	–	–	147	29.3	31.5
	1	200	61	1.7	82	9.9	148	30.0	21.6
	10	200	59	3.0	74	11.1	147	30.0	20.3
	100	200	60	5.9	74	10.4	147	29.6	20.6
	100-A*	200	59	–	–	–	147	27.8	29.0
	100	400	62	5.2	74	12.9	148	31.6	20.0
PLA98	nt	0	66	6.2	128	28.8	165	32.8	4.2
	nt-A	0	61	–	–	–	166	38.5	41.4
	1	200	62	0.5	81	3.7	165	38.9	37.8
	10	200	62	3.3	75	8.2	164	39.1	33.2
	100	200	62	3.9	74	10.5	164	41.5	33.4
	100-A*	200	64	–	–	–	164	37.3	40.1
	100	400	65	4.6	75	10.3	165	39.9	31.8

nt, nontested (original film); A, annealed at 110°C during 6 h; A*, annealed at 75 °C during 5 min.

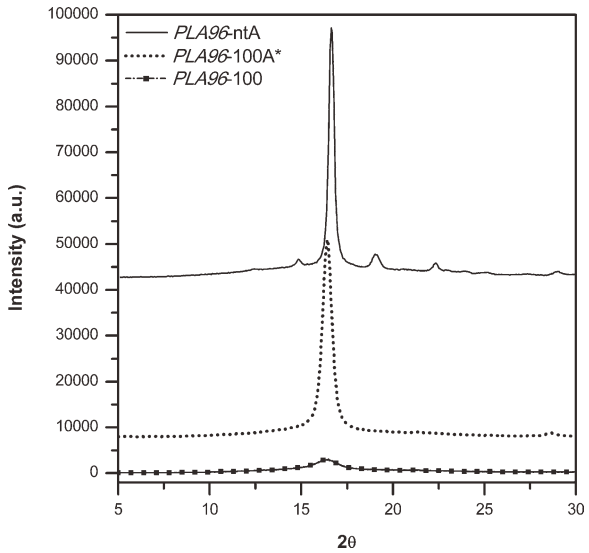

Figure 6. WAXS intensity profiles corresponding to PLA96 films: stretched (PLA96-100), stretched and annealed at 75°C (PLA96-100A*) and annealed at 110°C (PLA96-ntA).

temperatures barely above the T_g. Stretching of the films did not induce complete crystallization, but a semiordered state, with conformations close to those of crystals but without regular spacing. Such a state has been described by Stoclet et al. as a mesomorphic phase,[16,17] also found following uniaxial drawing of blown PLA films. Once the polymer chains achieve enough energy to move, the polymer chains in that mesomorphic phase rearrange their conformation to a crystal structure, with a smaller variation in energy than if the previous state was amorphous. Therefore, the exothermal peak considered by us as "cold crystallization" is instead the energy variation between this metastable state and the crystalline one, i.e., melting of the mesomorphic phase and further recrystallization.

For the sake of verifying this hypothesis, 200% stretched films at 100 mm/min were annealed at 75°C for 5 min (PLA96-100A* and PLA98-100A*) and analyzed by DSC (see Table II) and WAXS (Figure 6). Such a short annealing time and low temperature, compared with the typical annealing conditions for PLA recrystallization,[24] was enough to promote a great increase in crystallinity, as evidenced when the diffractograms are compared in Figure 6. This behavior indicates that in the stretched films, PLA chains present an ordered orientation, with conformations close to those of crystals, but with no regular spacing.

More evidence of this phenomenon can be found in the Fourier transformed infrared spectroscopy (FTIR) spectra of the films. It was observed that in the 970–835 cm^{-1} spectral range, there were some absorption bands that are related with to the crystal structure of PLA. The one at 923 cm^{-1} has been assigned to the coupling of the stretching C—C bond within the polymer chain with the rocking mode of the —CH_3 group. This band was then affected by the 10_3 helix conformation present in the α crystal structure of PLA. The absorption in this band in combination with the decrease in the band at 955 cm^{-1} has been related to PLA crystallization.[10,28,29] In Figure 7, several FTIR spectra are shown, corresponding to PLA96 films and postmortem tensile specimens.

It can be observed that the thermally annealed samples (PLA96-ntA and PLA96-100A*), with X_c values assessed by DSC around 30%, show a clear absorbance peak at 923 cm^{-1}. However, the stretched films, even though they showed X_c values around 20% in DSC, did not present their corresponding absorption peaks, because their spectra were more similar to the nonstretched films than to the highly crystalline ones.

Mechanical Behavior of Thermoformed (drawn) Films

To investigate the effect of thermoforming on the final properties of the films, uniaxial drawing simulated this process. Considering the results of the previous sections, the simulation was carried out at 70°C and 100 mm/min, with a draw extent of 200% and fast cooling. Tensile dumbbell specimens were punched from these oriented films for tensile and dynamomechanical thermal analysis (DMTA) characterization.

Effect on the Tensile Properties. Figure 8 shows the representative stress–strain curves from the stretched films (st-PLA96 and st-PLA98), obtained at 10 mm/min and 22°C. The curves corresponding to their respective original films are also included in Figure 8, for comparative purposes. A drastic change could be observed in the mechanical behavior of the stretched (thermoformed) films, where yielding occurred with localized neck formation. Next, the necked section propagated a uniform stress, which was higher than the yielding stress of the original films. Finally, a strain hardening effect could be identified, finding higher values of elongation at break than the original films. The failure in the stretched films took place with some tearing. Such behavior may be related to that of semicrystalline

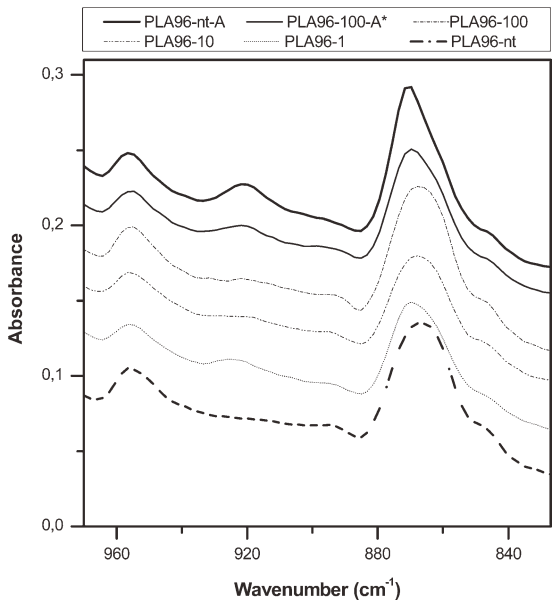

Figure 7. Section of the FTIR spectra corresponding to PLA96 films with different drawing conditions: nt represents nontested (original) films, A stands for thermally annealed films at 110°C for 6 h and A* indicates thermally annealed films at 75°C for 5 min).

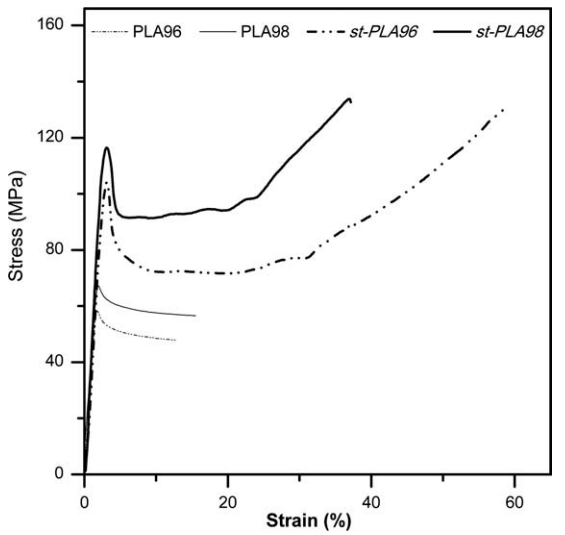

Figure 8. Tensile stress–strain curves for original and stretched films performed at 22°C and 10 mm/min.

polymers with processing-induced morphologies, where crystal structures are oriented along the testing direction.[8]

The tensile properties determined for st-PLA96 and st-PLA98 are shown in Table I, with their corresponding original films. Drawing not only produced a great increase in stiffness and yielding strength but also increased the deformation at yielding and deformation at break. It is well known that the tensile properties of semicrystalline polymers are highly dependent on the degree of crystallinity and the morphology/orientation of the crystalline domains.[8] Even though DSC tests showed an apparent increase in the crystallinity ratio promoted by drawing, which could account for an increase in E and σ_y, the values assessed for stretched PLA films were higher than those reported for PLA specimens with a similar crystallinity index but obtained by thermal annealing (E=4.1 GPa and σ_y=75.4 MPa),[5] in agreement with Stoclet et al. work.[17]

Comparing both PLA grades, the same trends in σ_y observed for the original films persisted in the stretched ones. However, differences in the elastic modulus and deformation at yielding arose. PLA98 showed higher E values than their corresponding PLA96 drawn films, but smaller values of ε_y. These differences are quite significant, revealing that the choice of a particular grade might not be trivial if the final application implies thermoforming with a high draw ratio.

Dynamomechanical Thermal Analysis. In a package, there can be some thermomechanical stresses during the sealing and/or hot filling stages, which may cause deformation and deterioration of the package. For this reason, packages are required to withstand such stresses without losing their shape. At the present, PS, poly(ethylene terephthalate), and isotactic polypropylene (i-PP), with typical elastic modules of 3.5, 3.1, and 1.5 GPa, respectively, are the most used materials for thermoforming. Hence, it can be reasonably assumed that a certain polymer that in a broad range of temperatures guarantees at least the stiffness of i-PP at room temperature (1.5 GPa) will be appropriate for packaging applications in such a temperature range.

In this work, an arbitrary value of storage modulus $E' = 2.2$ GPa has been considered as a fair value for typical packaging application purposes. By using this criterion, the thermomechanical resistance of different polymer films can be compared, evaluating at which temperature the elastic modulus decreases below that point. Such temperature in DMTA analysis has been defined as ($T_{2.2}$). The films with higher thermal resistance will show higher $T_{2.2}$ values.

Figure 9 shows the variation in the storage modulus (E') with temperature obtained by DMTA for both PLA grades before and after simulating the thermoforming process. It can be remarked that the E' values of the samples obtained at 30°C by DMTA are in agreement with the E values reported previously from mechanical tests. The same trends regarding the influence of the L-isomer content and orientation can be, hence, found and explained with the same arguments based on orientation and crystal structure. Figure 9 allows finding $T_{2.2}$ for all films; these values were 68°C and 69°C for PLA96 and PLA98 films (unstretched) and 70°C and 75°C for st-PLA96 and st-PL98 films, respectively.

When the temperature is close to T_g (around 65°C), a change in the dynamomechanical behavior can be viewed, characterized by a sharp drop in E'. In the case of unstretched films, such a drop reached a value of E' of 1 MPa and as the temperature continued to increase, then some of the stiffness was recovered, up to 10–20 MPa, which remained stable at that value until the melting temperature of PLA. Such behavior can be reasonably explained by an increase in crystallinity produced by the cold crystallization phenomenon analyzed by DSC and discussed previously.

However, the E' values for st-PLA96 and st-PLA98 films did not fall so low as their corresponding unstretched films, showing a rapid increase in E' at 90°C. Again, this behavior can be related with the information provided by DSC, WAXS, and FTIR. The stretched films showed a conformation close to that of a crystalline structure and, once the polymer chains acquired some

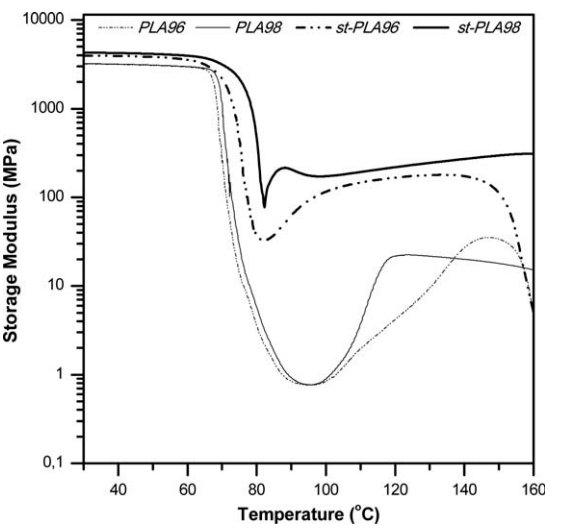

Figure 9. Variation in storage modulus (E') as a function of temperature for PLA films (original and stretched).

mobility, they rearranged rapidly, forming crystallites in a sort of nucleation-enhanced-crystallization.[30] It is wel known that crystallites act as anchor points, limiting the movements of the amorphous polymer sections.[31] In this case, because the grade with a higher L-isomer content (st-PLA98) developed higher crystallinity at higher rates, it showed better thermomechanical stability, with higher stiffness in the entire temperature range compared to st-PLA96.

CONCLUSIONS

The mechanical tests performed at different temperatures and crosshead rates with PLA films with different L-isomer contents showed that thermoforming simulation can be approached by tensile tests at 70°C and strain rates of 0.03–0.3 s^{-1}. Within the testing boundaries, it was shown that there is no influence of the PLA L-isomer content on the tensile parameters during drawing. Therefore, it can be assumed that replacing one grade with the other during industrial processing would not represent a dramatic change in the processing parameters.

Drawing at 70°C produces some structural rearrangements, with the formation of a mesomorphic phase, which is not purely crystalline, although it is stable at room temperature. The tensile properties of this phase (modulus, tensile strength, strain at yielding and break) increase with respect to the amorphous film. This mesomorphic phase, indeed, rearranges into a crystalline structure very rapidly at 75°C. The highest and fastest values of crystallinity were achieved with the highest L-isomer content PLA grade (PLA98).

Finally, it can be predicted that to produce thermally stable PLA products by thermoforming, it would be necessary to: (i) use a high L-isomer content PLA grade, (ii) use a processing temperature of 70°C and assure deformation rates of 0.3–0.03 s^{-1}, and (iii) add an annealing step at 75°C to maintain the shape of the product.

ACKNOWLEDGMENTS

The authors would like to thank the Ministerio de Educación y Ciencia for providing funds for the project MAT 2010-19721-C02-01, in which this work is involved. J. C. Velázquez-Infante also thanks the Agencia Española de Cooperación Internacional para el Desarrollo (AECID) for the grant of a pre-doctoral scholarship.

REFERENCES

1. Allard, R.; Charrier, J. M.; Ghosh, A.; Marangou, M.; Ryan, M. E.; Shrivastava, S.; Wu, R. *J Polym Eng* **1986,** *6*, 363.
2. Lim, L. T.; Auras, R.; Rubino, M. *Prog Polym Sci* **2008,** *33*, 820.
3. Wolf, O.; Crank, M.; Patel, M.; Marscheider-Weidemann, F. Techno-economic Feasibility of Large-scale Production of Bio-based Polymers in Europe. EUR No. 22103 EN. European Commission, **2005.**
4. Sarasua, J. R.; Arraiza, A. L.; Balerdi, P.; Maiza, I. *J Mater Sci* **2005,** *40*, 1855.
5. Carrasco, F.; Pages, P.; Gamez-Perez, J.; Santana, O. O.; Maspoch, M. L. *Polym Degrad Stab* **2010,** *95*, 116.
6. Gámez-Pérez, J.; Velazquez-Infante, J. C.; Franco-Urquiza, E.; Pages, P.; Carrasco, F.; Santana, O. O.; Maspoch, M. L. *Express Polym Lett* **2011,** *5*, 82.
7. Park, S. D.; Todo, M.; Arakawa, K. *J Mater Sci* **2005,** *40*, 1055.
8. Maspoch, M. L.; Gamez-Perez, J.; Gimenez, E.; Santana, O. O.; Gordillo, A. *J Appl Polym Sci* **2004,** *93*, 2866.
9. Gamez-Perez, J.; Munoz, P.; Santana, O. O.; Gordillo, A.; Maspoch, M. L. *J Appl Polym Sci* **2006,** *101*, 2714.
10. Lee, J. K.; Lee, K. H.; Jin, B. S. *Eur Polym J* **2001,** *37*, 907.
11. Solarski, S.; Ferreira, M.; Devaux, E. *J Text Inst* **2007,** *98*, 227.
12. Yu, L.; Liu, H. S.; Xie, F. W.; Chen, L.; Li, X. X. *Polym Eng Sci* **2008,** *48*, 634.
13. Okuzaki, H.; Kubota, I.; Kunugi, T. *J Polym Sci Part B: Polym Phys* **1999,** *37*, 991.
14. Aroujalian, A.; Ngadi, M. O.; Emond, J. P. *Polym Eng Sci* **1997,** *37*, 178.
15. Mezghani, K.; Spruiell, J. E. *J Polym Sci Part B: Polym Phys* **1998,** *36*, 1005.
16. Stoclet, G.; Seguela, R.; Lefebvre, J. M.; Li, S.; Vert, M. *Macromolecules* **2011,** *44*, 4961.
17. Stoclet, G.; Seguela, R.; Lefebvre, J. M.; Rochas, C. *Macromolecules* **2010,** *43*, 7228.
18. Available at: http://www.natureworksllc.com. Accessed on October 30, 2010.
19. Fischer, E. W.; Sterzel, H. J.; Wegner, G. *Kolloid Zeitschrift Zeitschrift Fur Polym* **1973,** *251*, 980.
20. Arefazar, A.; Hay, J. N. *Polymer* **1982,** *23*, 1129.
21. Cowie, J. M. G.; Harris, S.; McEwen, I. J. *Macromolecules* **1998,** *31*, 2611.
22. Kolstad, J. J. *J Appl Polym Sci* **1996,** *62*, 1079.
23. Mahendrasingam, A.; Blundell, D. J.; Parton, M.; Wright, A. K.; Rasburn, J.; Narayanan, T.; Fuller, W. *Polymer* **2005,** *46*, 6009.
24. Nascimento, L.; Gamez-Perez, J.; Santana, O. O.; Velasco, J. I.; Maspoch, M. L.; Franco-Urquiza, E. *J Polym Environ* **2010,** *18*, 654.
25. Goto, K.; Nakano, S.; Kuriyama, T. *Strength Fract Complex* **2006,** *4*, 185.
26. Ayhan, Z.; Zhang, Q. H. *Polym Eng Sci* **2000,** *40*, 1.
27. Todo, M.; Park, S. D.; Arakawa, K. *J Mater Sci* **2004,** *39*, 1113.
28. Kister, G.; Cassanas, G.; Vert, M. *Polymer* **1998,** *39*, 267.
29. Sawai, D.; Takahashi, K.; Sasashige, A.; Kanamoto, T.; Hyon, S. H. *Macromolecules* **2003,** *36*, 3601.
30. Aou, K.; Kang, S. H.; Hsu, S. L. *Macromolecules* **2005,** *38*, 7730.
31. Cicero, J. A.; Dorgan, J. R.; Janzen, J.; Garrett, J.; Runt, J.; Lin, J. S. *J Appl Polym Sci* **2002,** *86*, 2828.